Chemical Science

ROYAL SOCIETY OF CHEMISTRY

EDGE ARTICLE

View Article Online
View Journal | View Issue

Cite this: *Chem. Sci.*, 2023, **14**, 149

All publication charges for this article have been paid for by the Royal Society of Chemistry

Received 20th September 2022
Accepted 21st November 2022

DOI: 10.1039/d2sc05229f

rsc.li/chemical-science

Sensitizer-controlled photochemical reactivity *via* upconversion of red light†

Felix Glaser and Oliver S. Wenger *

By combining the energy input from two red photons, chemical reactions that would normally require blue or ultraviolet irradiation become accessible. Key advantages of this biphotonic excitation strategy are that red light usually penetrates deeper into complex reaction mixtures and causes less photo-damage than direct illumination in the blue or ultraviolet. Here, we demonstrate that the primary light-absorber of a dual photocatalytic system comprised of a transition metal-based photosensitizer and an organic co-catalyst can completely alter the reaction outcome. Photochemical reductions are achieved with a copper(I) complex in the presence of a sacrificial electron donor, whereas oxidative substrate activation occurs with an osmium(II) photosensitizer. Based on time-resolved laser spectroscopy, this changeover in photochemical reactivity is due to different underlying biphotonic mechanisms. Following triplet energy transfer from the osmium(II) photosensitizer to 9,10-dicyanoanthracene (DCA) and subsequent triplet–triplet annihilation upconversion, the fluorescent singlet excited state of DCA triggers oxidative substrate activation, which initiates the *cis* to *trans* isomerization of an olefin, a [2 + 2] cycloaddition, an aryl ether to ester rearrangement, and a Newman–Kwart rearrangement. This oxidative substrate activation stands in contrast to the reactivity with a copper(I) photosensitizer, where photoinduced electron transfer generates the DCA radical anion, which upon further excitation triggers reductive dehalogenations and detosylations. Our study provides the proof-of-concept for controlling the outcome of a red-light driven biphotonic reaction by altering the photosensitizer, and this seems relevant in the greater context of tailoring photochemical reactivities.

Introduction

Conventional photoreactions typically aim at one catalytic turnover per absorbed photon, but recently many new applications of multi-photon excitation strategies in photoredox catalysis were developed.[1] In these cases, two (or more) photons are required per catalytic turnover, but thermodynamically unusually challenging reactions become accessible as a result of the combined energy input from multiple photons. Most systems investigated in this context operate on the basis of a single photocatalyst, for example involving consecutive photoinduced electron transfer (conPET),[2–10] photoionization processes,[11,12] structural *in situ* catalyst modifications,[13–15] or light-driven catalyst recovery.[16,17] The combination of a photoredox catalyst with a co-catalyst is less common,[18,19] and combinations of two photoactive catalysts are yet very scarce.[20,21,22,39]

Sensitized triplet–triplet annihilation upconversion (sTTA-UC) is an attractive approach to combining the energy input of multiple photons.[1,23–25] In this case, the co-catalyst (the so-called annihilator) is not directly excited, but instead its lowest triplet excited state is formed *via* triplet–triplet energy transfer (TTET) from the primary photosensitizer and then the annihilator's fluorescent singlet excited state is populated by triplet–triplet annihilation. That singlet excited state can either activate the substrate directly, or it can be quenched by sacrificial electron donors to yield a radical anion, which subsequently engages with the substrate.[24] Direct photo-excitation of the respective singlet excited state of the annihilator would typically require ultraviolet excitation, and consequently the main advantage of the sTTA-UC strategy is that much lower-energy input radiation can be employed. In the recent past, different upconversion systems relying on blue,[24,26,27] green,[28–30] red,[31] or near-infrared excitation sources[32–35] were developed for applications in photo(redox) catalysis. With rare exceptions,[33] mainly reductive dehalogenations have been reported until now, typically in the presence of a sacrificial amine donor, sometimes complemented by a radical trapping reagent. This limited reaction scope stands in contrast to the very large diversity of light-driven reactions relying on monophotonic mechanisms.[36] It seems surprising that almost exclusively reductive substrate activations have been investigated so far by

Department of Chemistry, University of Basel, St. Johanns-Ring 19, 4056 Basel, Switzerland. E-mail: oliver.wenger@unibas.ch

† Electronic supplementary information (ESI) available. See DOI: https://doi.org/10.1039/d2sc05229f

multi-photonic excitation mechanisms, whereas only few oxidative transformations have been targeted.[37,38]

Recently, we reported a new strategy for reductive dehalogenations and detosylations based on red light irradiation (Fig. 1h) by combining $[Cu(dap)_2]^+$ (dap = 2,9-dianisyl-1,10-phenanthroline) together with 9,10-dicyanoanthracene (DCA).[39] The involved mechanism resembled the Z-scheme of natural photosynthesis, and this represents a potentially widely applicable concept for multi-photonic catalysis. In this previous study, photoinduced electron transfer from $[Cu(dap)_2]^+$ generated DCA radical anions ($DCA^{\bullet-}$), which engaged in reductive substrate activation upon further excitation. In the present study, we targeted oxidative substrate activations from the fluorescent singlet excited state of DCA (^{1*}DCA), which has a very high oxidation potential of +1.99 V *vs.* SCE.[40] There have been many previous reports on photocatalytic applications of DCA[41–49] and related cyanoarenes,[40] though usually involving direct ultraviolet or blue excitation. Here, we targeted the formation of ^{1*}DCA *via* upconversion of red light, to accomplish chemical transformations requiring high oxidative potentials, contrasting our recent studies, in which excitation of $DCA^{\bullet-}$ led to thermodynamically challenging reductions under red irradiation.[39] In other words, the goal was to completely reverse the photoredox reactivity of a biphotonic reaction system with DCA a key catalytic component.

The idea of controlling and switching the reaction outcome by changing the conditions in photo(redox) catalysis has obtained attention mostly for monophotonic mechanisms until now.[50] For example, the change of the photocatalyst from $[Ru(bpy)_3]^{2+}$ to *fac*-$[Ir(ppy)_3]$ led to different products for the reaction of trifluoromethyl iodide with an alkyne (Fig. 1a).[51] In other studies, the reaction conditions rather than the catalyst played a key role in controlling the change of the formed photoproducts, for example the reaction time (Figure 1b),[52] the temperature (Figure 1c),[53] the use of additives (Figure 1d),[54] or co-catalysts (Fig. 1e).[55] Furthermore, a change of the excitation wavelength (Fig. 1f)[5] and the irradiation light intensity (Fig. 1g)[56] have been found to alter the achievable photoreactions by switching between monophotonic and biphotonic excitation. However, apart from these two latter examples, divergent photochemical reactivities of biphotonic systems have been less in focus,[12] presumably due to their inherently high overall complexity.

Against this background, we were curious whether we could revert the reactivity of the photosensitizer/DCA combination from the previously observed highly reducing behaviour (involving $DCA^{\bullet-}$), to strong oxidizing reactivity (based on ^{1*}DCA) as noted above, while keeping red light as a low-energy irradiation source. We envisioned that sTTA-UC would give access to the strongly oxidizing ^{1*}DCA, which should be readily possible with red light given the low triplet energy of ~1.8 eV of ^{3*}DCA.[57] Thus, instead of the previously exploited photoinduced electron transfer (PET) from $[Cu(dap)_2]^+$ to DCA,[39] we targeted TTET as an initial elementary reaction step, and this required a different primary photosensitizer which replaces $[Cu(dap)_2]^+$. In other words, we aimed to actively change the mechanism of a biphotonic reaction by altering the photosensitizer (Fig. 1h).

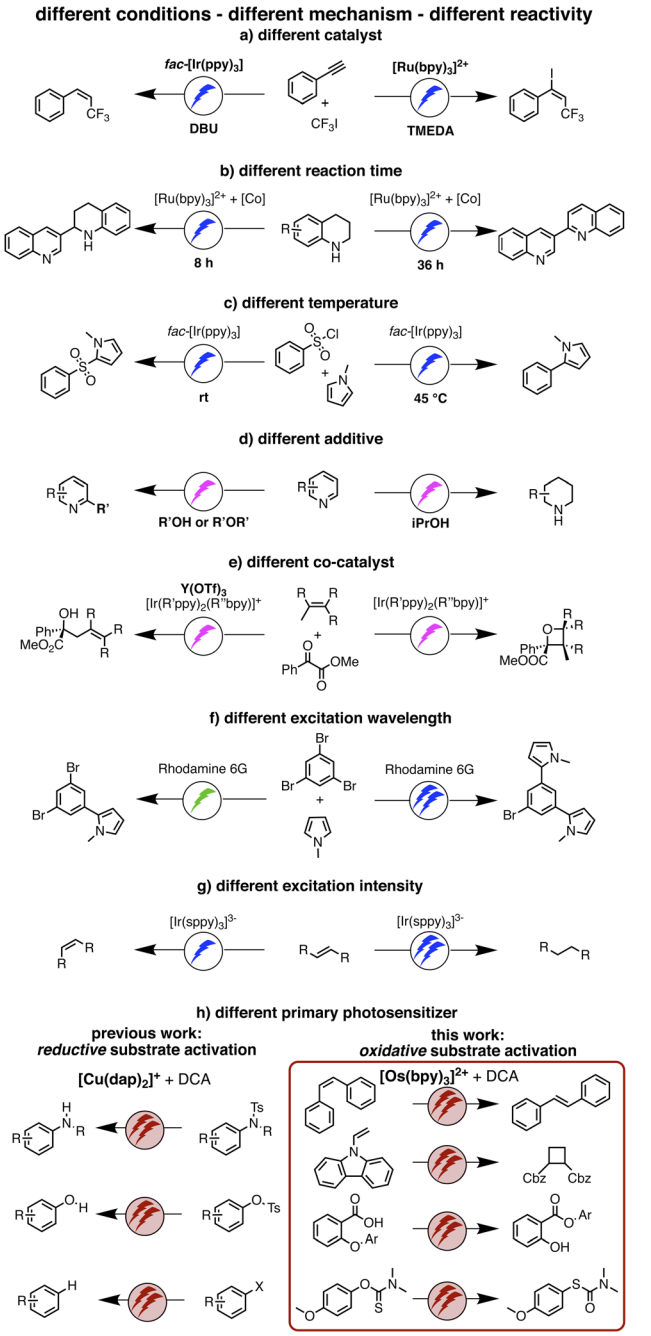

Fig. 1 (a–g) Previously reported examples of light-driven reactions with changes of reaction conditions to achieve different photochemical reaction outcomes, mostly relying on monophotonic (blue or green) excitation.[5,51–56] (h) Our work on reductive substrate activation[39] and oxidative substrate activation with red light (this work). Depending on whether the primary photosensitizer is a Cu^{I} or an Os^{II} polypyridine complex, different biphotonic reaction mechanisms are operative, and either very negative reduction potentials (left) or very positive oxidation potentials are accessible (right).

Detailed mechanistic insight into all light-driven reaction steps is the key to understanding observable photochemical reactivities,[24,58–68] and here such understanding provides the basis for the targeted active reaction control.

The number of photocatalysts with suitable absorption properties in the red spectral range is somewhat limited,[31,69–72] and we chose a well-known polypyridyl complex of osmium(II) from as class of robust sensitizers that have been used successfully for triplet–triplet annihilation previously.[73–79] In combination with DCA, the change from $[Cu(dap)_2]^+$ to $[Os(bpy)_3]^{2+}$ as a primary light absorber completely alters the photochemical reactivity of the system. With the copper(I) sensitizer in the presence of a sacrificial electron donor, we observed the reductive activation of substrates requiring potentials below −2.0 V *vs.* SCE, whereas with the osmium(II) sensitizer the oxidative activation of substrates requiring potentials close to +2.0 V *vs.* SCE is achievable. The specific reactions explored herein are four different overall redox-neutral reactions that all rely on an initial light-induced substrate oxidation step initiated by ^{1*}DCA (Fig. 1h).

Results and discussion

Triplet–triplet annihilation upconversion

In a first set of experiments we explored whether the combination of DCA and $[Os(bpy)_3]^{2+}$ is indeed suitable for our purposes. In principle, sTTA-UC is well established for many anthracene derivatives,[76,80–83] and TTET from $[Os(bpy)_3]^{2+}$ to DCA is expected to be thermodynamically viable based on the relevant triplet energies.[39,57] On the other hand, a more thorough analysis suggests that photoinduced electron transfer could in principle compete (detailed discussion in Section 4.2.2 of the ESI†), hence the anticipated TTET (and ensuing upconversion) reactivity cannot be taken for granted. Transient UV-vis absorption spectroscopy provides unambiguous evidence for ^{3*}DCA as the only detectable photoproduct formed directly upon quenching of $[Os(bpy)_3]^{2+}$, hence TTET is clearly the dominant reaction pathway of excited $^{3*}[Os(bpy)_3]^{2+}$. In the following, the TTA upconversion properties were investigated in acetonitrile, acetone and dichloromethane. Less polar solvents were not considered due to anticipated challenges associated with photoinduced charge separation and enhanced exciplex formation (see below).[84–91]

The choice of solvent can play an important role for the performance of an upconversion system,[92–94] and in our case solubility issues had to be considered. In very polar solvents, the solubility of DCA decreases, while in more apolar solvents the charged osmium(II) complex becomes less soluble. The solubility of the DCA annihilator is the more important factor, due to the higher concentrations needed of this component in comparison to the sensitizer.

The rate constants for energy transfer from $^{3*}[Os(bpy)_3]^{2+}$ to DCA (k_{TTET}) and for the triplet–triplet annihilation (k_{TTA}) are both largely independent on the solvent (Table 1). Due to the abovementioned differences in solubility and different excited state properties of the osmium(II) sensitizer (*e.g.* the lifetime τ_0 change from 94 ns in dichloromethane to 61 ns in acetonitrile), a direct comparison of the determined upconversion quantum yield ($\Phi_{sTTA\text{-}UC}$) in different solvents is not straightforward. However, a clear trend to better upconversion quantum yields in less polar solvents is found. Specifically, the respective quantum yield is ~1.5% in dichloromethane (with respect to a theoretical maximum of 50%, Fig. 2a and b) whereas in acetone and acetonitrile values of ~0.13% and ~0.22%, respectively, are achievable (Table 1). The main reason for these discrepant $\Phi_{sTTA\text{-}UC}$ values is most likely the substantially higher solubility of DCA in dichloromethane, leading to more efficient excited-state quenching of the osmium(II) sensitizer by TTET. Even in the case of dichloromethane with 3 mM of dissolved DCA (used for the determination of $\Phi_{sTTA\text{-}UC}$ in Table 1), less than 50% of $^{3*}[Os(bpy)_3]^{2+}$ is quenched ($k_{TTET}\cdot[DCA]/(k_{TTET}\cdot[DCA] + {\tau_0}^{-1}) = (3 \times 10^9\ M^{-1}\ s^{-1} \times 3\ mM)/(3 \times 10^9\ M^{-1}\ s^{-1} \times 3\ mM + (94\ ns)^{-1}) \approx 46\%$). Thus, the solubility of DCA limits the overall achievable upconversion quantum yield (further discussion in Section 4.3.3 of the ESI†). In the other investigated solvents, the DCA solubility is only ~0.5 mM (Table 1), and consequently the resulting TTET efficiency is further diminished.

As expected for a biphotonic process, a quadratic dependence of the DCA upconversion fluorescence intensity on the excitation power density is found (Fig. 2c, blue). At elevated excitation power densities, the change towards an approximately linear regime with a slope of 1.35 on a double logarithmic scale (Fig. 2c, red) indicates that the so-called strong annihilation limit is reached. From the intersection between the (approximately) quadratic and linear fits, a threshold of ~1.65 W cm^{-2} can be estimated. A reference experiment without annihilator revealed almost perfectly linear power

Table 1 Summary of different photophysical properties of the sTTA-UC system comprised of $[Os(bpy)_3]^{2+}$ and DCA in different solvents[a]

Solvent	$k_{TTET}/M^{-1}\ s^{-1}$	$k_{TTA}/M^{-1}\ s^{-1}$	[DCA]/mM	λ_{ex}/nm	$\Phi_{sTTA\text{-}UC}$[b]/%	ΔE[b]/eV
Acetonitrile	4×10^9	6.9×10^9	0.5	635	~0.22	0.88
				705	~0.10	1.06
Acetone	4×10^9	6.4×10^9	0.5	635	~0.13	0.88
				705	~0.15	1.08
Dichloromethane	3×10^9	6.7×10^9	3	635	~1.5	0.73
				705	~1.4	0.92

[a] The data were recorded in de-aerated solvents. Details for the determination of the triplet–triplet energy transfer rate constant k_{TTET}, the triplet–triplet annihilation rate constant k_{TTA}, the sensitized triplet–triplet annihilation upconversion quantum yield $\Phi_{sTTA\text{-}UC}$ and the apparent pseudo anti-Stokes shifts ΔE are in the ESI in Sections 4.2 and 4.3. [b] The pseudo anti-Stokes shift and the upconversion quantum yield were determined using the concentrations of DCA indicated in the table. The concentration of $[Os(bpy)_3](PF_6)_2$ was different for excitation with a 635 nm cw laser (20 μM) and a 705 nm cw laser excitation (50 μM).

dependence of the prompt osmium(II) photoluminescence with a slope of 0.97 (Section 4.3.2 in the ESI†).

In all three investigated solvents (weak) excimer emission is detectable under upconversion conditions, manifesting in an emission band extending up to ~650 nm (ESI, Section 4.3.2†). In acetonitrile and acetone the highest-energy DCA fluorescence peak around 440 nm (corresponding to the 0–0 transition) is clearly detectable under upconversion conditions, whereas in dichloromethane this band is not detectable anymore due to inner filter effects caused by the higher concentration in this solvent (Fig. 2a).[95] Thus, the delayed fluorescence band maximum in dichloromethane corresponds to the first vibrational progression member of the prompt DCA fluorescence and consequently, the apparent pseudo anti-Stokes shift for dichloromethane is 0.73 eV, while in acetone and acetonitrile the emission maximum is 0.88 eV higher in energy than the excitation wavelength (Table 1, see ESI Section 4.3.2† for details). Using excitation at 705 nm instead of 635 nm, similar upconversion quantum yields $\Phi_{sTTA\text{-}UC}$ remain achievable (Table 1),[34] but now pseudo anti-Stokes shifts over 1 eV result (Table 1). While systems with significantly better upconversion quantum yields are known,[80,96–102] our apparent pseudo anti-Stokes shifts are close to current state of the art.[31,76,94,98,101,103,104]

Since the highest upconversion quantum yield was obtained in dichloromethane, the long-term photostability was studied in this specific solvent (Fig. 2d). Irradiation over 5 hours revealed that our photosensitizer/annihilator combination is very robust and essentially no loss in the upconversion intensity is detectable (blue trace). Unsurprisingly, the reference without annihilator revealed that the osmium(II)-based sensitizer is also very photostable (red trace). Even after 14 days of irradiating a reaction mixture with a red cw laser, the characteristic signals of the sensitizer as well as the annihilator remain easily detectable by ^{1}H-NMR spectroscopy (ESI Section 4.8.5†). These measurements indicate a good photostability of our sensitizer/catalyst combination under long-term red irradiation. Overall, these properties seem useful for the application of the $[Os(bpy)_3]^{2+}$/DCA combination for photoredox catalysis *via* upconversion.

Cis–trans photo-isomerisation of stilbene

Isomerisation reactions of stilbenes sensitized by direct blue or UV excitation of DCA have long been known to proceed through a mechanism involving stilbene radical cations.[87,105,109–114] The prototypical example is the photo-isomerisation of *cis*-stilbene (**1**) to *trans*-stilbene (**1-P**),[105,109,111] and this reaction seemed promising for our proof-of-concept study involving upconversion of red light, particularly because this is a simple reaction for which comparatively fast substrate conversion can be anticipated on the basis of the previous UV irradiation studies.[109] First reactions with 5 mol% of DCA under blue LED irradiation (440 nm, 40 W) in acetonitrile and dichloromethane resulted in conversions of over 75% within 1 hour (see ESI Table S1 and Fig. S1†). In dichloromethane ~85% of **1-P** are present in the photostationary state,[107] while in acetonitrile the reactant is essentially completely converted to product.[109]

For initial tests with red light irradiation in the presence of 1 mol% of $[Os(bpy)_3]^{2+}$, a collimated high-power 623 nm LED (min. 3.8 W) was used to drive the reaction on an NMR scale (Fig. 3, ESI Section 2.3†). In contrast to what is observed under

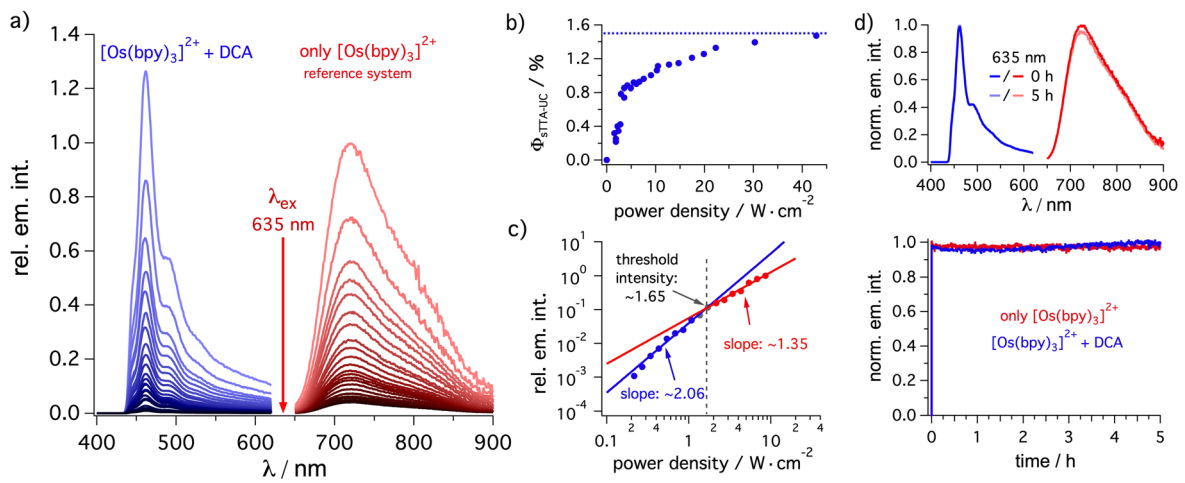

Fig. 2 Triplet–triplet annihilation upconversion analysis. (a) Steady-state emission spectra of $[Os(bpy)_3](PF_6)_2$ (20 μM) in de-aerated dichloromethane at 20 °C excited at 635 nm with a cw laser using different excitation densities in the absence of DCA (red, reference system) and upconverted delayed fluorescence spectra in the presence of DCA (3 mM) under otherwise identical conditions. (b) Upconversion quantum yield ($\Phi_{sTTA\text{-}IC}$) determination based on the data in (a) using the emission quantum yield of $[Os(bpy)_3](PF_6)_2$ (2.7%, determined against $[Ru(bpy)_3]^{2+}$ in a separate experiment) as reference system. (c) Determination of the threshold for the changeover from the quadratic excitation power dependence to a nearly linear regime, based on the integrated upconversion fluorescence intensity of DCA (3 mM) sensitized by $[Os(bpy)_3](PF_6)_2$ (20 μM) in de-aerated dichloromethane (ESI Section 4.3.2†). (d) Photostability of $[Os(bpy)_3](PF_6)_2$ (50 μM) (red trace) and of the $[Os(bpy)_3](PF_6)_2$ (50 μM)/DCA (3 mM) upconversion system (blue trace) under 635 nm cw laser excitation (450 mW). The upconverted emission was detected at 460 nm while the prompt sensitizer emission was detected at 720 nm (ESI Section 4.3.5†). The upper part of this panel contains the emission spectra of both solutions before and after 5 hours of irradiation.

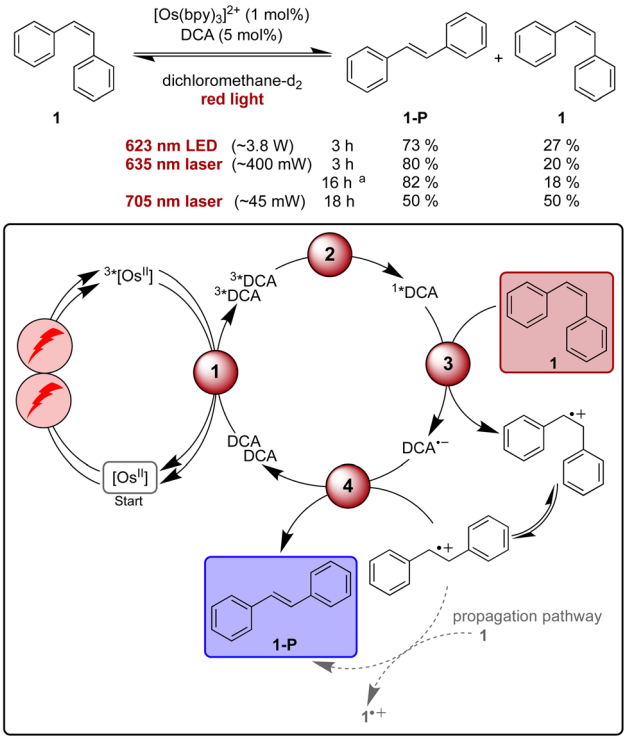

Fig. 3 Light-driven isomerisation of *cis*-stilbene (**1**) under red-light irradiation along with a plausible mechanism involving triplet–triplet energy transfer (1), triplet–triplet annihilation upconversion (2), substrate activation (3), and catalyst recovery (4). Main steps of substrate activation adapted from a known monophotonic mechanism.[105] A radical chain propagation pathway is plausible for this reaction (details in text and ESI Section 4.8.3†),[106] and further intermediates (for example a transient dimer radical cation) can be involved.[107–109] All yields were determined by ^{1}H-NMR spectroscopy using 1,4-dioxane as internal standard. Further information is in Section 4.4 of the ESI.†

blue irradiation above, the reaction progress depended strongly on the solvents. In acetonitrile-d_3, only 18% product formation was observed after 2 hours while in dichloromethane-d_2 61% of **1-P** were detected after the same irradiation time (ESI, Fig. S1†). This finding is in line with the significantly higher triplet–triplet annihilation upconversion quantum yield in dichloromethane compared to acetonitrile. In the latter solvent, 96% formation of *trans*-stilbene required a much longer irradiation time of 40 hours (ESI, Table S2†).

As our spectroscopic investigations indicated a threshold intensity around 1.65 W cm^{-2} (Fig. 2c) for the changeover from quadratic to linear dependence of the upconversion process, excitation with a cw laser rather than a LED was tested in the next step. The cw laser power is lower (~400 mW) compared to the LED (min. 3.8 W, further discussion in ESI Section 2.3.1†), yet the laser source gave a slightly better product yield (80% of **1-P**) compared to 73% after 3 h of irradiation with the collimated LED for NMR-scale reactions (Fig. 3). Thus, the laser irradiation setup, which provides a higher power density, due to the more collimated nature of the laser beam, was used for further investigations. With prolonged irradiation times of 16 h, the loading of $[Os(bpy)_3]^{2+}$ could be lowered to 0.1 mol% (Fig. 3), resulting in a turnover number of over 1500 with respect to the photosensitizer.

Contrary to previous studies,[109] following direct excitation of DCA at 405 nm in the absence of sensitizer and under otherwise identical conditions as for the sensitized catalysis, no clear evidence for a propagation pathway was found neither in acetonitrile (photochemical quantum yield Φ_{PC} ~0.13) nor in dichloromethane (Φ_{PC} ~0.03, ESI Section 4.8.3†) under the conditions used herein. An experiment with our upconversion system under red-light irradiation results in an only slightly smaller value for the quantum yield of *cis*- to *trans*-stilbene isomerization in dichloromethane (Φ_{PC} ~0.015), which is close to the triplet–triplet annihilation upconversion quantum yield in that solvent (Table 1). It does not seem plausible that every successful upconversion event leads to product, and therefore contributions from a radical chain mechanism under upconversion conditions seem likely (ESI Section 4.8.3†). When using a comparatively low-power 705 nm cw laser (~45 mW), 50% of the substrate was converted to the *trans*-isomer after 18 hours of irradiation (Fig. 1). As for all other investigated light-driven transformations reported herein, no product formation was observed in the absence of light or any of the catalysts (ESI Tables S3–S8†).

Mechanistic investigations reveal that photoinduced electron transfer from *cis*-stilbene **1** to ^{1*}DCA (1.46×10^{10} M^{-1} s^{-1} in dichloromethane) as well as from the *trans*-stilbene product **1-P** to ^{1*}DCA (1.54×10^{10} M^{-1} s^{-1}) are both essentially diffusion-limited (the diffusion limit in dichloromethane at 20 °C is 1.5×10^{10} M^{-1} s^{-1}).[57,109] Direct substrate activation by triplet energy transfer from $^{3*}[Os(bpy)_3]^{2+}$, by reductive quenching of $^{3*}[Os(bpy)_3]^{2+}$ or by quenching of ^{3*}DCA are not important for the observed reactivity in our system (ESI Section 4.4†). Consequently, the mechanism involving triplet–triplet annihilation upconversion presented in Fig. 3 (including direct oxidation of **1** as well as contributions from a radical chain propagation pathway) is suggested as the main contributor for product formation in this red-light driven isomerisation reaction.

Carbon–carbon bond formation *via* [2 + 2] cycloaddition

Functionalization of radical cations and [2 + 2] cycloaddition reactions catalysed by pyrylium salts or DCA as photocatalysts have been reported previously.[42,87,116–119] One of the challenges associated with [2 + 2] cycloadditions of alkenes is the reversibility of the overall process, due to a possible (unwanted) ring-opening reaction of the formed product.[116] Therefore, the use of a redox mediator can be advantageous to selectively activate the substrate whilst preventing the undesirable backward reaction of the cycloaddition product.[116,120] 9-Vinylcarbazole (**2**) has been found to undergo successful [2 + 2] cycloaddition sensitized by an organic dye in the absence of a redox mediator, and therefore this specific substrate was selected as model compound for our proof-of-principle studies.[116]

Starting with direct blue excitation (440 nm LED, 40 W) of ^{1*}DCA in acetone, 80% of product **2-P** were formed in 0.5 hours (ESI Fig. S2 and Table S3†), whereas only 19% of **2-P** (Table S3†)

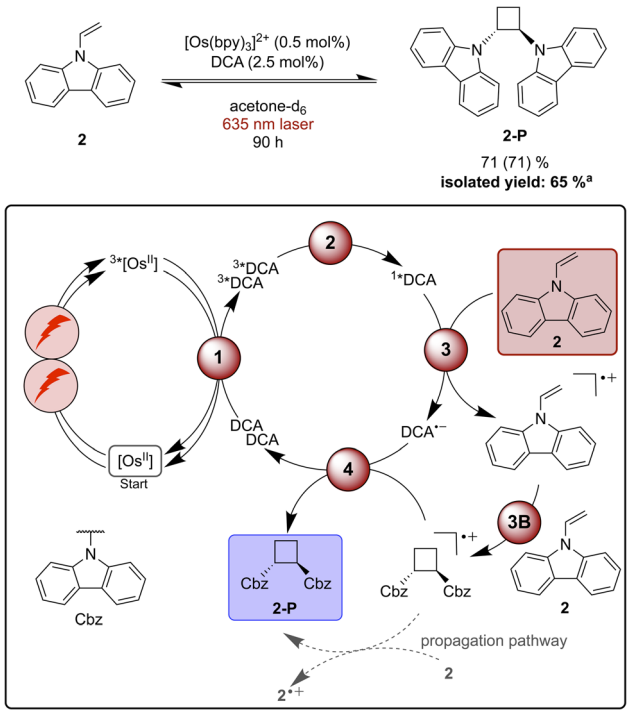

Fig. 4 [2 + 2] Cycloaddition of vinylcarbazole (**2**) under red-light irradiation and a plausible mechanism involving triplet–triplet energy transfer (1), triplet–triplet annihilation upconversion (2), substrate activation (3), cycloaddition (3B), and catalyst recovery (4). Main steps of substrate activation adapted from a previously reported monophotonic mechanism.[106,115,116] A radical chain propagation pathway is likely for this reaction (details in text and ESI Section 4.8.3†).[106] The yield (conversion in parenthesis) was determined by ^{1}H-NMR spectroscopy using 1,4-dioxane as internal standard. Further information is in Section 4.5 of the ESI.† [a]Product isolation was performed on a 400 μmol scale of **2** under 623 nm LED irradiation.

formed in dichloromethane under identical conditions. Consequently, acetone was used for the reaction under red cw laser irradiation, despite the markedly lower upconversion yield in this solvent (Table 1). Under 635 nm laser irradiation the reaction becomes significantly slower and 90 hours are needed to achieve 71% product formation (Fig. 4), presumably due to the low upconversion quantum yield in acetone. Based on the comparison of the quantum yield for the photochemical [2 + 2] cycloaddition reaction and $\Phi_{sTTA\text{-}UC}$, a radical chain propagation pathway is likely to contribute under red light irradiation (ESI Section 4.8.3†).[106]

Unwanted quenching of triplet-excited DCA or direct ^{3}MLCT quenching of the osmium(II) sensitizer by the substrate are inefficient based on spectroscopic investigations (ESI Section 4.5†). The proposed mechanism for the formation of product **2-P** (Fig. 4) is similar to the stilbene isomerisation discussed above, except of course for the cycloaddition step between the radical cation and one equivalent of unreacted substrate (step 3B in Fig. 4).[116,121]

When using a 623 nm LED (min. 3.8 W) instead of the 635 nm cw laser, a larger volume can be irradiated, and the reaction can be performed better on somewhat enlarged scale (ESI Section 4.3†).[120] Using 0.5 mol% sensitizer and 2.5 mol% of DCA in acetone, the reaction was performed on a 400 μmol scale and **2-P** was isolated with a yield of 65% after 90 hours of irradiation. This example demonstrates that in principle upconversion with red light is useable for (small-scale) preparative reactions with (collimated) LED irradiation – a light source that is typically more available in synthetic laboratories than cw lasers.

Newman–Kwart rearrangement

Newman–Kwart rearrangements have previously been investigated by chemical,[125] photochemical[122,124] and electrochemical[123] approaches involving single-electron substrate oxidation. This represents an attractive alternative way for this reaction to occur under mild conditions compared to thermal activation, which typically requires temperatures between 200 °C and 300 °C.[126] Fast substrate oxidation with pyrylium salts and detailed mechanistic studies have been reported previously, providing a helpful basis for our investigations of red light driven Newman–Kwart rearrangement.[122,124]

Initial experiments focusing on the direct formation of ^{1*}DCA with blue light revealed that both naphthalene and $TBAPF_6$ (tetra-*n*-butylammonium hexafluorophosphate) are necessary additives in dichloromethane to accomplish the Newman–Kwart rearrangement of substrate **3** in acceptable yields (see ESI Table S5† for details). Under $[Os(bpy)_3]^{2+}$ sensitized conditions with 635 nm laser irradiation the reaction became markedly slower, and after 20 hours a yield of 10% for the rearrangement product **3-P** was found for a reaction on NMR scale. Essentially linear product formation as a function time was observed (ESI Fig. S3†), and after 14 days of irradiation 88% of rearranged product **3-P** was obtained (Fig. 5). This indicates a very good long-term stability of our upconversion system, in line with the short-term investigations in Fig. 2d. A more potent irradiation source in combination with a flow setup would be desirable to accelerate this reaction,[127] but the proof of principle is now made.

Pulsed laser experiments and UV-vis transient absorption spectroscopy under upconversion conditions in the presence of naphthalene provide no clear evidence for oxidized naphthalene and reduced DCA, most likely because the overall process is inefficient and because there are spectrally overlapping signals with ^{3*}DCA. However, an unexpected ground-state absorption bleach appears between 450 and 700 nm in the presence of naphthalene. A comparison to spectro-electrochemical data indicates that this bleach signals the interim formation of $[Os(bpy)_3]^{3+}$ (ESI Section 4.8.4†), suggesting a cascade reactivity to form $DCA^{\bullet-}$ and $Nap^{\bullet+}$ after TTA-UC, followed by subsequent electron transfer from $[Os(bpy)_3]^{2+}$ to $Nap^{\bullet+}$. This latter step represents an unwanted deactivation pathway, which can serve as a plausible explanation for the slow reaction progress observed under red light driven upconversion conditions, in addition to the low sTTA-UC quantum yield. Based on the mechanistic insights gained here, it seems reasonable to assume that this deactivation pathway involving sensitizer oxidation generally contributes to the observable significantly

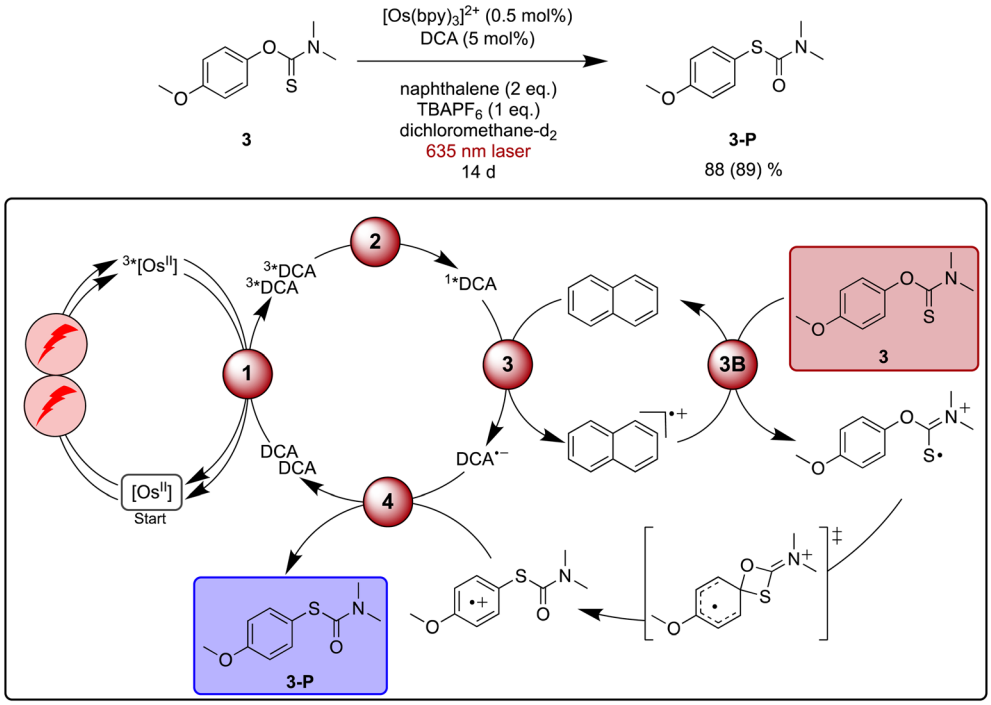

Fig. 5 Light-driven Newman–Kwart rearrangement of substrate **3** under red-light irradiation, along with a plausible mechanism including triplet–triplet energy transfer (1), triplet–triplet annihilation upconversion (2), excited state quenching by naphthalene mediator (3), substrate activation (3B), and catalyst recovery (4). The main steps of substrate activation are analogous those postulated previously for a monophotonic mechanism.[122,123] A possible radical chain propagation pathway and previously proposed off-cycle intermediates are omitted for simplicity.[122–124] Yield (conversion in parenthesis) was determined by ^{1}H-NMR spectroscopy against 1,4-dioxane as internal standard. Further information is in Section 4.6 of the ESI.†

prolonged reaction times when using upconversion from the red instead of direct blue DCA excitation.

Based on the abovementioned previous Newman–Kwart rearrangement studies involving single electron transfer,[122–124] a simplified mechanism for our upconversion system including a naphthalene-mediated pathway is proposed in Fig. 5. Previous studies of related reactions in acetonitrile furthermore proposed a radical chain propagation pathway as well as off-cycle intermediates, which are not considered here for simplicity.[122–124]

Ether-to-ester rearrangement

As a final reaction example, the rearrangement of the aryl ether **4** to aryl ester **4-P** *via* aryl migration was explored. This reaction has been previously reported with perylene diimide or acridinium salts as photocatalysts under blue irradiation in the presence of a sub-stoichiometric amount of base.[128–130] The base is necessary to facilitate substrate oxidation, which in this case occurs from the deprotonated carboxylate (**4**$^-$). Similar to what was found above for the Newman–Kwart rearrangement reaction, $TBAPF_6$ helps accelerate product formation in dichloromethane upon direct excitation of DCA with blue light (Table S7†), and several different bases provided good results. However, with aliphatic amines such as 1,8-diazabicyclo(5.4.0) undec-7-ene (DBU, +1.24 V *vs.* SCE)[131] or triethylamine (+0.69 V *vs.* SCE)[132] unwanted reductive quenching of ^{1*}DCA (+1.99 V *vs.* SCE),[3,133] or even reductive quenching of ^{3*}DCA can potentially occur.[39] Consequently, 2,4,6-trimethylpyridine (tMePy, 2.25 V *vs.* SCE, ESI Section 4.1.4†) was chosen. Expectedly, the quenching of ^{1*}DCA by tMePy is two orders below the diffusion limit (10^8 M^{-1} s^{-1}), and our reaction optimisation experiments under blue irradiation (440 nm LED, 40 W) indicated that a stoichiometric amount of tMePy is beneficial (ESI Table S7†).

Under irradiation with a 635 nm cw laser, the NMR scale rearrangement of ether **4** to 64% of ester **4-P** required 140 h, while 81% of starting material was consumed. Isolation of the product on a slightly larger scale with a 623 nm LED resulted in a yield of 75% after the same reaction time.

Time-resolved experiments indicate that ^{1*}DCA is quenched by **4**$^-$ with a rate constant of 5×10^9 M^{-1} s^{-1}, whereas no DCA fluorescence quenching is detectable without substrate deprotonation (ESI Section 4.7†). Control experiments monitoring the photoluminescence of $[Os(bpy)_3]^{2+}$ provide evidence for static quenching, manifesting in a shortened decay time independent of the concentration of **4**$^-$. This suggests that $[Os(bpy)_3]^{2+}$ and **4**$^-$ aggregate, which possibly opens an unwanted deactivation pathway that could lead to diminished product formation under upconversion conditions compared to direct excitation of DCA with blue light. However, the addition of salt seems to counteract this deactivation by diminishing unwanted aggregation (ESI Section 4.7.2†). Control experiments confirm that DCA is an indispensable component for the red light driven

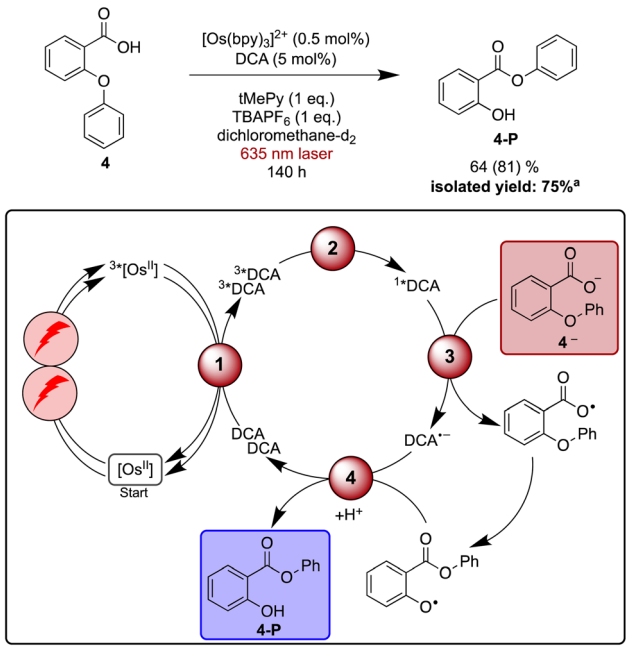

Fig. 6 Red light-driven ether-to-ester rearrangement of substrate **4** along with a plausible mechanism including triplet–triplet energy transfer (1), triplet–triplet annihilation upconversion (2), substrate activation (3), and catalyst recovery (4). Main steps of substrate activation adapted from a previously published monophotonic mechanism.[128] Yield (conversion in parenthesis) was determined by ^{1}H-NMR spectroscopy using 1,4-dioxane as internal standard. Further information is in Section 4.7 of the ESI.† [a]Product isolation was performed on a 250 μmol scale of **4** under 623 nm LED irradiation.

reaction (Table S8†), hence photoexcited $[Os(bpy)_3]^{2+}$ seems to be unable to oxidize $\mathbf{4}^-$ in catalytically relevant amounts.

General mechanistic aspects

The four investigated proof-of-principle reactions reported above provide direct insight into what factors and processes affect the efficiency of biphotonic reactions in comparison to traditional monophotonic mechanisms. First, the optimal reaction conditions are not necessarily identical for both excitation strategies. This finding is illustrated by the photoisomerisation of *cis*- to *trans*-stilbene, where the limited solubility and the resulting low triplet–triplet annihilation upconversion quantum yield clearly affect the overall reaction progress over time. While under blue light irradiation comparable reaction progress has been found in different solvents, under upconversion conditions significant differences in reaction progress are observed. Second, when two (photo)catalysts are present, additional (unwanted) deactivation steps can occur. Our time-resolved spectroscopic investigations of the naphthalene-mediated rearrangement of substrate **3**, where the naphthalene radical cation intermediate was found to be partially deactivated in an unproductive pathway by electron transfer from the $[Os(bpy)_3]^{2+}$ sensitizer, illustrate this aspect. Third, as illustrated by the ether-to-ester rearrangement in Fig. 6, aggregation of a negatively charged substrate with the cationic photosensitizer is possible in apolar solvents, and the addition of salt can become important to minimize deactivation of the photosensitizer in an unwanted side reaction (Fig. 5 and 6). All of these aspects need to be considered in biphotonic mechanisms (Fig. 7), in addition to complications that are already present under monophotonic excitation conditions. Specifically, this includes unproductive pathways such as excimer and exciplex formation, as well as unproductive excited state deactivation by intersystem crossing to ^{3*}DCA, or direct decay of ^{1*}DCA to the ground state (ESI Sections 4.8.1 and 4.8.4†).[134–136]

On the other hand, radical chain propagation pathways can contribute substantially to the overall reaction efficiency and seem to play important roles for at least two of the four investigated reactions herein. Furthermore, our studies suggest that improved cage escape yields to form solvent separated radical ions are achievable by the addition of salt, and the use of redox mediators for electron transfer cascade pathways is beneficial for some of the upconversion-driven photoreactions. Many of these effects can differ significantly based on exact conditions (solvent, additive, reaction type), and our work indicates that complementary UV-vis transient absorption and time-resolved luminescence spectroscopic investigations can provide particularly valuable insights when targeting biphotonic excitation strategies. Some of the challenges outlined above could potentially be tackled with higher annihilator concentrations[78] (for

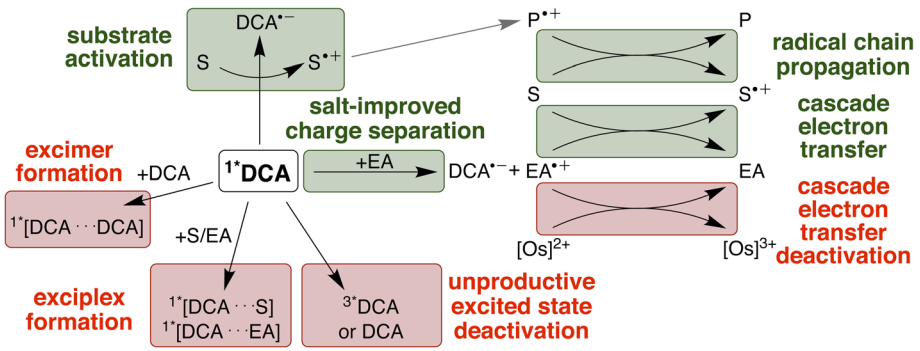

Fig. 7 Summary of productive and unproductive pathways for the deactivation of ^{1*}DCA after triplet–triplet annihilation upconversion. EA = electron acceptor/mediator; S = substrate; P = product. Favourable processes are coloured in green, unwanted processes in red.

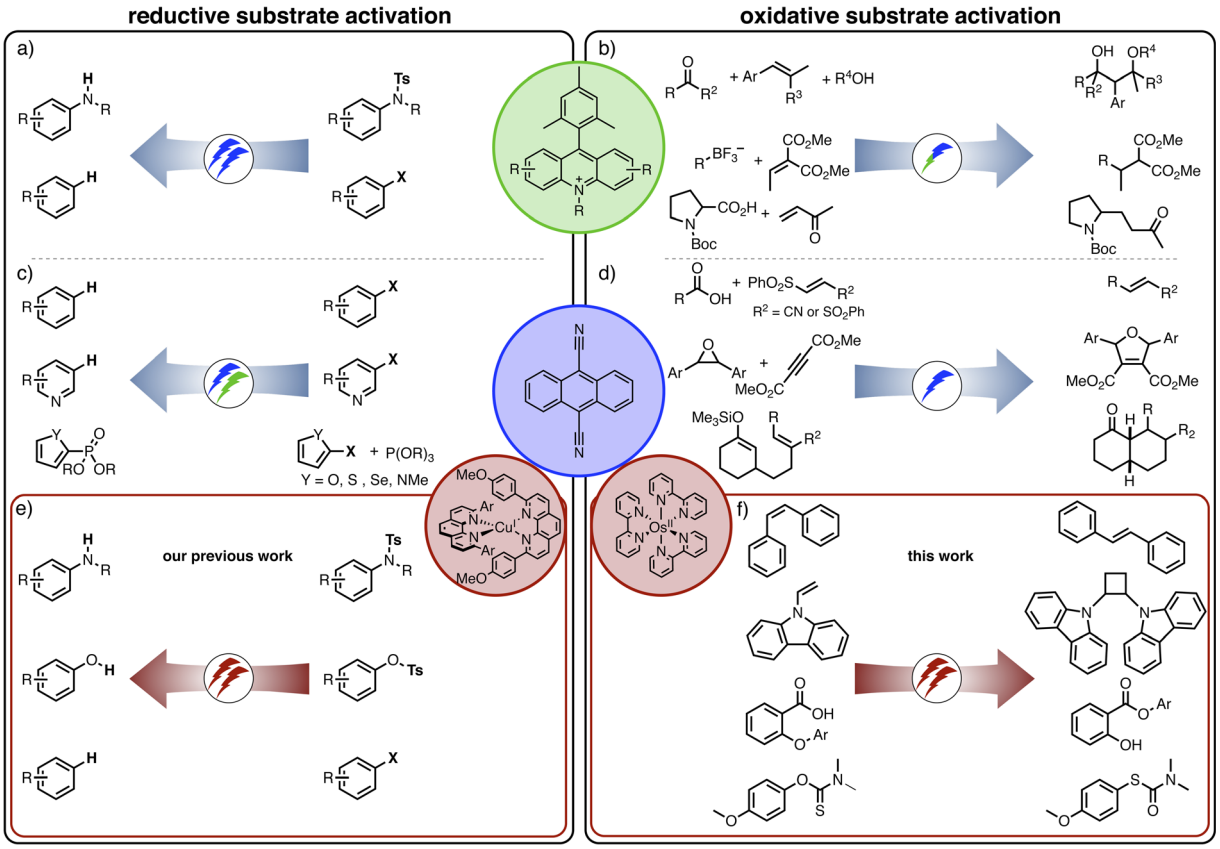

Fig. 8 Selected examples of different approaches to oxidative and reductive substrate activation with acridinium dyes and direct (monophotonic) blue/green light (a and b),[4,140–142] direct excitation of DCA in the blue or green spectral range (c and d),[3,9,42,43,119] and two-catalyst systems operating under red light irradiation (e and f).[39] Overall redox-neutral reactions requiring an initial substrate oxidation step have been chosen on the right-hand side of the figure.

example with modified DCA structures)[49] or photosensitizers with longer lifetimes.[80,98] Any enhancement of the sTTA-UC quantum yield would likely substantially improve the achievable photochemical quantum yield under red light irradiation in our system (ESI Section 4.8.3†). To counteract unwanted cascade deactivations, different catalysts[137–139] or chemical environments[8,21,61] might be promising. The main productive and unproductive pathways for the deactivation of ^{1*}DCA are summarized in Fig. 7 (further discussion in ESI Section 4.8†).

Conclusions

Biphotonic excitation strategies for photoredox catalysis have received growing attention within the last few years, and many different mechanisms have been considered.[1] Until now, most biphotonic reaction approaches rely on a single light absorber (acridinium dyes in Fig. 8a, DCA in Fig. 8c). Recently, we explored a reaction system comprised of two different light absorbers, where we observed photoinduced electron transfer from a Cu^{I} photosensitizer to DCA, and subsequent (secondary) excitation of $DCA^{\bullet-}$ led to thermodynamically challenging reductive dehalogenations and detosylations (Fig. 8e).[39] In the present study, the use of an Os^{II} photosensitizer leads to triplet–triplet energy transfer to DCA and ensuing upconversion, and the resulting highly oxidizing ^{1*}DCA (instead of $DCA^{\bullet-}$) induces the photochemical reactions of interest (Fig. 8f).

Conceptually, this changeover in photochemical reactivity (Fig. 8e and f) is related to the changeover between oxidative and reductive substrate activation with acridinium salts (Fig. 8a and b)[4,143] under direct (monophotonic) blue excitation, or *via* consecutive photoinduced electron transfer (ConPET) using DCA[3,40] or perylene diimide (PDI)[40] under blue and green irradiation (Fig. 8c and d). Similar reactivity changes might become achievable with other systems, and the idea of investigating new photochemical mechanisms rather than developing new catalysts could become more important in the future.[38] Increasing attention to elucidate mechanisms will be helpful in this context.[24,58,59,62,68,80,144–151] Mechanistic studies seem particularly desirable for oxidative substrate activation, for several reasons. First, reductive dehalogenations often involve a fast and irreversible bond cleavage step,[152] whereas oxidative substrate activations can be reversible reactions. Second, low cage escape yields for photogenerated radical pairs, unwanted back-electron transfer, and deactivation *via* electron transfer cascades are typically less important (or at least less in focus)[146,153] for reductive transformations, but have to be considered carefully for oxidative transformations originating from singlet excited states (Fig. 7).[38,49,116,154–156]

The development of new red or near-infrared light absorbing catalysts could potentially give access to new photochemical applications with low-energy input light.[31,79,120,151,157–164] Furthermore, recent interest in triplet–triplet annihilation upconversion will likely promote the development of more sophisticated systems with lower threshold irradiation intensities that permit more effective excitation by LEDs, higher photochemical quantum yields and larger pseudo anti-Stokes shifts,[34,76,78,96,100,104,165] resulting in more efficient setups for applications in photo(redox) catalysis in the future.[166,167] We hope that the concepts and proof-of-principle reactions presented herein can serve as useful inspiration for future catalytic applications with red and near-infrared light.[9,23,163,168–170]

Data availability

All experimental data, procedures for data analysis and pertinent data sets are provided in the ESI.† All electronic data is available on **https://Zenodo.org**.

Author contributions

F. G. conceived the project, designed photochemical studies, carried out spectroscopic, synthetic and electrochemical work, analysed data and performed photocatalytic measurements; O. S. W. conceived the project and provided guidance. The manuscript was written through contributions of all authors.

Conflicts of interest

There are no conflicts to declare.

Acknowledgements

This work was funded by the Swiss National Science Foundation through grant number 200020_207329. Björn Pfund is acknowledged for helpful discussions.

References

1 F. Glaser, C. Kerzig and O. S. Wenger, *Angew. Chem., Int. Ed.*, 2020, **59**, 10266–10284.
2 I. Ghosh, T. Ghosh, J. I. Bardagi and B. König, *Science*, 2014, **346**, 725–728.
3 M. Neumeier, D. Sampedro, M. Májek, V. A. de la Peña O'Shea, A. Jacobi von Wangelin and R. Pérez-Ruiz, *Chem.–Eur. J.*, 2018, **24**, 105–108.
4 I. A. MacKenzie, L. Wang, N. P. R. Onuska, O. F. Williams, K. Begam, A. M. Moran, B. D. Dunietz and D. A. Nicewicz, *Nature*, 2020, **580**, 76–80.
5 I. Ghosh and B. König, *Angew. Chem., Int. Ed.*, 2016, **55**, 7676–7679.
6 R. Naumann, F. Lehmann and M. Goez, *Angew. Chem., Int. Ed.*, 2018, **57**, 1078–1081.
7 R. Naumann, C. Kerzig and M. Goez, *Chem. Sci.*, 2017, **8**, 7510–7520.
8 M. Giedyk, R. Narobe, S. Weiß, D. Touraud, W. Kunz and B. König, *Nat. Catal.*, 2020, **3**, 40–47.
9 J. C. Herrera-Luna, D. D. Díaz, M. C. Jiménez and R. Pérez-Ruiz, *ACS Appl. Mater. Interfaces*, 2021, **13**, 48784–48794.
10 J. Soika, C. McLaughlin, T. Neveselý, C. G. Daniliuc, J. J. Molloy and R. Gilmour, *ACS Catal.*, 2022, **12**, 10047–10056.
11 T. Kohlmann, R. Naumann, C. Kerzig and M. Goez, *Photochem. Photobiol. Sci.*, 2017, **16**, 1613–1622.
12 C. Kerzig, X. Guo and O. S. Wenger, *J. Am. Chem. Soc.*, 2019, **141**, 2122–2127.
13 J. P. Cole, D.-F. Chen, M. Kudisch, R. M. Pearson, C.-H. Lim and G. M. Miyake, *J. Am. Chem. Soc.*, 2020, **142**, 13573–13581.
14 H. Li, X. Tang, J. H. Pang, X. Wu, E. K. L. Yeow, J. Wu and S. Chiba, *J. Am. Chem. Soc.*, 2021, **143**, 481–487.
15 T. U. Connell, C. L. Fraser, M. L. Czyz, Z. M. Smith, D. J. Hayne, E. H. Doeven, J. Agugiaro, D. J. D. Wilson, J. L. Adcock, A. D. Scully, D. E. Gómez, N. W. Barnett, A. Polyzos and P. S. Francis, *J. Am. Chem. Soc.*, 2019, **141**, 17646–17658.
16 Y. Qiao, Q. Yang and E. J. Schelter, *Angew. Chem., Int. Ed.*, 2018, **57**, 10999–11003.
17 P. W. Antoni and M. M. Hansmann, *J. Am. Chem. Soc.*, 2018, **140**, 14823–14835.
18 I. Ghosh, R. S. Shaikh and B. König, *Angew. Chem., Int. Ed.*, 2017, **56**, 8544–8549.
19 M. S. Coles, G. Quach, J. E. Beves and E. G. Moore, *Angew. Chem., Int. Ed.*, 2020, **59**, 9522–9526.
20 A. Hu, Y. Chen, J.-J. Guo, N. Yu, Q. An and Z. Zuo, *J. Am. Chem. Soc.*, 2018, **140**, 13580–13585.
21 C. Kerzig and M. Goez, *Chem. Sci.*, 2016, **7**, 3862–3868.
22 A. Chinchole, M. A. Henriquez, D. Cortes-Arriagada, A. R. Cabrera and O. Reiser, *ACS Catalysis*, 2022, **12**(21), 13549–13554.
23 R. Pérez-Ruiz, *Top. Curr. Chem.*, 2022, **380**, 23.
24 F. Glaser, C. Kerzig and O. S. Wenger, *Chem. Sci.*, 2021, **12**, 9922–9933.
25 J. Castellanos-Soriano, D. Álvarez-Gutiérrez, M. C. Jiménez and R. Pérez-Ruiz, *Photochem. Photobiol. Sci.*, 2022, **21**, 1175–1184.
26 M. Majek, U. Faltermeier, B. Dick, R. Pérez-Ruiz and A. Jacobi von Wangelin, *Chem.–Eur. J.*, 2015, **21**, 15496–15501.
27 T. J. B. Zähringer, J. A. Moghtader, M.-S. Bertrams, B. Roy, M. Uji, N. Yanai and C. Kerzig, *Angew. Chem., Int. Ed.*, 2022, e202215340.
28 M. Häring, R. Pérez-Ruiz, A. J. Von Wangelin and D. D. Díaz, *Chem. Commun.*, 2015, **51**, 16848–16851.
29 C. Kerzig and O. S. Wenger, *Chem. Sci.*, 2018, **9**, 6670–6678.
30 S. Liu, H. Liu, L. Shen, Z. Xiao, Y. Hu, J. Zhou, X. Wang, Z. Liu, Z. Li and X. Li, *Chem. Eng. J.*, 2022, **431**, 133377.
31 J. B. Bilger, C. Kerzig, C. B. Larsen and O. S. Wenger, *J. Am. Chem. Soc.*, 2021, **143**, 1651–1663.
32 M. Freitag, N. Möller, A. Rühling, C. A. Strassert, B. J. Ravoo and F. Glorius, *ChemPhotoChem*, 2019, **3**, 24–27.

33 B. D. Ravetz, A. B. Pun, E. M. Churchill, D. N. Congreve, T. Rovis and L. M. Campos, *Nature*, 2019, **565**, 343–346.
34 L. Huang, W. Wu, Y. Li, K. Huang, L. Zeng, W. Lin and G. Han, *J. Am. Chem. Soc.*, 2020, **142**, 18460–18470.
35 L. Huang, L. Zeng, Y. Chen, N. Yu, L. Wang, K. Huang, Y. Zhao and G. Han, *Nat. Commun.*, 2021, **12**, 122.
36 C. K. Prier, D. A. Rankic and D. W. C. MacMillan, *Chem. Rev.*, 2013, **113**, 5322–5363.
37 D. Rombach and H. A. Wagenknecht, *Angew. Chem., Int. Ed.*, 2020, **59**, 300–303.
38 K. Targos, O. P. Williams and Z. K. Wickens, *J. Am. Chem. Soc.*, 2021, **143**, 4125–4132.
39 F. Glaser and O. S. Wenger, *JACS Au*, 2022, **2**, 1488–1503.
40 N. A. Romero and D. A. Nicewicz, *Chem. Rev.*, 2016, **116**, 10075–10166.
41 C. Yang, J.-D. Yang, Y.-H. Li, X. Li and J.-P. Cheng, *J. Org. Chem.*, 2016, **81**, 12357–12363.
42 E. Alfonzo, F. S. Alfonso and A. B. Beeler, *Org. Lett.*, 2017, **19**, 2989–2992.
43 L. M. Kammer, B. Lipp and T. Opatz, *J. Org. Chem.*, 2019, **84**, 2379–2392.
44 Y. Matsui, T. Ikeda, Y. Takahashi, M. Kamata, M. Akagi, Y. Ohya, R. Fujino, H. Namai, E. Ohta, T. Ogaki, T. Miyashi, S. Tero-Kubota, K. Mizuno and H. Ikeda, *Asian J. Org. Chem.*, 2017, **6**, 458–468.
45 Z. L. Wang, J. Chen, Y. H. He and Z. Guan, *J. Org. Chem.*, 2021, **86**, 3741–3749.
46 H. T. Qin, X. Xu and F. Liu, *ChemCatChem*, 2017, **9**, 1409–1412.
47 G. Pandey and R. Laha, *Angew. Chem., Int. Ed.*, 2015, **54**, 14875–14879.
48 P. A. Waske and J. Mattay, *Tetrahedron*, 2005, **61**, 10321–10330.
49 M. J. P. Mandigma, J. Žurauskas, C. I. MacGregor, L. J. Edwards, A. Shahin, L. D'Heureuse, P. Yip, D. J. S. Birch, T. Gruber, J. Heilmann, M. P. John and J. P. Barham, *Chem. Sci.*, 2022, **13**, 1912–1924.
50 Y. Sakakibara and K. Murakami, *ACS Catal.*, 2022, **12**, 1857–1878.
51 N. Iqbal, J. Jung, S. Park and E. J. Cho, *Angew. Chem.*, 2014, **126**, 549–552.
52 Z. Jia, Q. Yang, L. Zhang and S. Luo, *ACS Catal.*, 2019, **9**, 3589–3594.
53 S. K. Pagire, A. Hossain and O. Reiser, *Org. Lett.*, 2018, **20**, 648–651.
54 T. McCallum, S. P. Pitre, M. Morin, J. C. Scaiano and L. Barriault, *Chem. Sci.*, 2017, **8**, 7412–7418.
55 J. Zheng, X. Dong and T. P. Yoon, *Org. Lett.*, 2020, **22**, 6520–6525.
56 C. Kerzig and O. S. Wenger, *Chem. Sci.*, 2019, **10**, 11023–11029.
57 M. Montalti, A. Credi, L. Prodi and M. T. Gandolfi, *Handbook of Photochemistry*, CRC Press, Third edn, 2006.
58 B. G. Stevenson, E. H. Spielvogel, E. A. Loiaconi, V. M. Wambua, R. V. Nakhamiyayev and J. R. Swierk, *J. Am. Chem. Soc.*, 2021, **143**, 8878–8885.
59 C. J. Zeman, S. Kim, F. Zhang and K. S. Schanze, *J. Am. Chem. Soc.*, 2020, **142**, 2204–2207.
60 N. A. Till, L. Tian, Z. Dong, G. D. Scholes and D. W. C. MacMillan, *J. Am. Chem. Soc.*, 2020, **142**, 15830–15841.
61 R. Fayad, S. Engl, E. O. Danilov, C. E. Hauke, O. Reiser and F. N. Castellano, *J. Phys. Chem. Lett.*, 2020, **11**, 5345–5349.
62 L. Tian, N. A. Till, B. Kudisch, D. W. C. MacMillan and G. D. Scholes, *J. Am. Chem. Soc.*, 2020, **142**, 4555–4559.
63 Y. Zhang, T. S. Lee, J. L. Petersen and C. Milsmann, *J. Am. Chem. Soc.*, 2018, **140**, 5934–5947.
64 J. P. Menzel, B. B. Noble, J. P. Blinco and C. Barner-Kowollik, *Nat. Commun.*, 2021, **12**, 1691.
65 S. Gisbertz, S. Reischauer and B. Pieber, *Nat. Catal.*, 2020, **3**, 611–620.
66 F. Glaser, C. B. Larsen, C. Kerzig and O. S. Wenger, *Photochem. Photobiol. Sci.*, 2020, **19**, 1035–1041.
67 T. Noël and E. Zysman-Colman, *Chem Catal.*, 2022, **2**, 468–476.
68 L. Buzzetti, G. E. M. Crisenza and P. Melchiorre, *Angew. Chem., Int. Ed.*, 2019, **58**, 3730–3747.
69 K. Watanabe, N. Terao, I. Kii, R. Nakagawa, T. Niwa and T. Hosoya, *Org. Lett.*, 2020, **22**, 5434–5438.
70 H. Janeková, M. Russo, U. Ziegler and P. Štacko, *Angew. Chem.*, 2022, **134**, e202204391.
71 C. Grundke, R. C. Silva, W. R. Kitzmann, K. Heinze, K. T. De Oliveira and T. Opatz, *J. Org. Chem.*, 2022, **87**, 5630–5642.
72 L. Mei, J. M. Veleta and T. L. Gianetti, *J. Am. Chem. Soc.*, 2020, **142**, 12056–12061.
73 Y. Sasaki, M. Oshikawa, P. Bharmoria, H. Kouno, A. Hayashi-Takagi, M. Sato, I. Ajioka, N. Yanai and N. Kimizuka, *Angew. Chem., Int. Ed.*, 2019, **58**, 17827–17833.
74 Y. Sasaki, S. Amemori, H. Kouno, N. Yanai and N. Kimizuka, *J. Mater. Chem. C*, 2017, **5**, 5063–5067.
75 D. Liu, Y. Zhao, Z. Wang, K. Xu and J. Zhao, *Dalton Trans.*, 2018, **47**, 8619–8628.
76 Y. Wei, M. Zheng, L. Chen, X. Zhou and S. Liu, *Dalton Trans.*, 2019, **48**, 11763–11771.
77 D. Wei, X. Li, L. Shen, Y. Ding, K. Liang and C. Xia, *Org. Chem. Front.*, 2021, **8**, 6364–6370.
78 R. Haruki, Y. Sasaki, K. Masutani, N. Yanai and N. Kimizuka, *Chem. Commun.*, 2020, **56**, 7017–7020.
79 Z. Yuan, J. He, Z. Mahmood, L. Xing, S. Ji, Y. Huo and H. L. Zhang, *Dyes Pigm.*, 2022, **199**, 110049.
80 C. Wang, F. Reichenauer, W. R. Kitzmann, C. Kerzig, K. Heinze and U. Resch-Genger, *Angew. Chem., Int. Ed.*, 2022, **61**, e202202238.
81 S. Baluschev, T. Miteva, V. Yakutkin, G. Nelles, A. Yasuda and G. Wegner, *Phys. Rev. Lett.*, 2006, **97**, 7–9.
82 A. Olesund, V. Gray, J. Mårtensson and B. Albinsson, *J. Am. Chem. Soc.*, 2021, **143**, 5745–5754.
83 D. Dzebo, K. Moth-Poulsen and B. Albinsson, *Photochem. Photobiol. Sci.*, 2017, **16**, 1327–1334.
84 R. C. Kanner and C. S. Foote, *J. Am. Chem. Soc.*, 1992, **114**, 678–681.
85 A. F. Olea, D. R. Worrall and F. Wilkinson, *Photochem. Photobiol. Sci.*, 2003, **2**, 212–217.

86 A. F. Olea, D. R. Worrall, F. Wilkinson, S. L. Williams and A. A. Abdel-Shafi, *Phys. Chem. Chem. Phys.*, 2002, **4**, 161–167.
87 E. Hasegawa, K. Okada, H. Ikeda, Y. Yamashita and T. Mukai, *J. Org. Chem.*, 1991, **56**, 2170–2178.
88 S. L. P. Chang and D. I. Schuster, *J. Phys. Chem.*, 1987, **91**, 3644–3649.
89 Y. Takahashi, K. Wakamatsu, K. Kikuchi and T. Miyashi, *J. Phys. Org. Chem.*, 1990, **3**, 509–518.
90 M. Ottolenghi, C. R. Goldschmidt and R. Potashnik, *J. Phys. Chem.*, 1971, **75**, 1025–1031.
91 K. Kikuchi, M. Hoshi, T. Niwa, Y. Takahashi and T. Miyashi, *J. Phys. Chem.*, 1991, **95**, 38–42.
92 C. Ye, V. Gray, J. Mårtensson and K. Börjesson, *J. Am. Chem. Soc.*, 2019, **141**, 9578–9584.
93 Q. Zhou, M. Zhou, Y. Wei, X. Zhou, S. Liu, S. Zhang and B. Zhang, *Phys. Chem. Chem. Phys.*, 2017, **19**, 1516–1525.
94 Y. Murakami, A. Motooka, R. Enomoto, K. Niimi, A. Kaiho and N. Kiyoyanagi, *Phys. Chem. Chem. Phys.*, 2020, **22**, 27134–27143.
95 Y. Zhou, F. N. Castellano, T. W. Schmidt and K. Hanson, *ACS Energy Lett.*, 2020, **5**, 2322–2326.
96 A. Olesund, J. Johnsson, F. Edhborg, S. Ghasemi, K. Moth-Poulsen and B. Albinsson, *J. Am. Chem. Soc.*, 2022, **144**, 3706–3716.
97 X. Cao, B. Hu and P. Zhang, *J. Phys. Chem. Lett.*, 2013, **4**, 2334–2338.
98 N. Nishimura, V. Gray, J. R. Allardice, Z. Zhang, A. Pershin, D. Beljonne and A. Rao, *ACS Mater. Lett.*, 2019, **1**, 660–664.
99 M. Uji, N. Harada, N. Kimizuka, M. Saigo, K. Miyata, K. Onda and N. Yanai, *J. Mater. Chem. C*, 2022, **10**, 4558–4562.
100 W. Sun, A. Ronchi, T. Zhao, J. Han, A. Monguzzi and P. Duan, *J. Mater. Chem. C*, 2021, **9**, 14201–14208.
101 Y. Wei, Y. Li, M. Zheng, X. Zhou, Y. Zou and C. Yang, *Adv. Opt. Mater.*, 2020, **8**, 1902157.
102 Z. A. VanOrman and L. Nienhaus, *Matter*, 2021, **4**, 2625–2626.
103 C. Fan, L. Wei, T. Niu, M. Rao, G. Cheng, J. J. Chruma, W. Wu and C. Yang, *J. Am. Chem. Soc.*, 2019, **141**, 15070–15077.
104 T. J. B. Zähringer, M.-S. Bertrams and C. Kerzig, *J. Mater. Chem. C*, 2022, **10**, 4568–4573.
105 F. D. Lewis, A. M. Bedell, R. E. Dykstra, J. E. Elbert, I. R. Gould and S. Farid, *J. Am. Chem. Soc.*, 1990, **112**, 8055–8064.
106 R. A. Crellin, M. C. Lambert and A. Ledwith, *J. Chem. Soc. D*, 1970, 682.
107 Y. Kuriyama, H. Sakuragi, K. Tokumaru, Y. Yoshida and S. Tagawa, *Bull. Chem. Soc. Jpn.*, 1993, **66**, 1852–1855.
108 B. W. Zhang, Y. Kuriyama, Y. Cao and K. Tokumaru, *Bull. Chem. Soc. Jpn.*, 1993, **66**, 1859–1862.
109 F. D. Lewis, J. R. Petisce, J. D. Oxman and M. J. Nepras, *J. Am. Chem. Soc.*, 1985, **107**, 203–207.
110 T. Tamai, N. Ichinose, T. Tanaka, T. Sasuga, I. Hashida and K. Mizuno, *J. Org. Chem.*, 1998, **63**, 3204–3212.
111 F. D. Lewis, R. E. Dykstra, I. R. Gould and S. Farid, *J. Phys. Chem.*, 1988, **92**, 7042–7043.
112 K. Mizuno, N. Ichinose and Y. Otsuji, *Chem. Lett.*, 1985, **14**, 455–458.
113 K. Mizuno, N. Ichinose and Y. Otsuji, *J. Org. Chem.*, 1992, **57**, 1855–1860.
114 Y. Kuriyama, T. Arai, H. Sakuragi and K. Tokumaru, *Chem. Lett.*, 1992, **21**, 879–882.
115 S. Mckinley, J. V. Crawford and C. H. Wang, *J. Org. Chem.*, 1966, **31**, 1963–1964.
116 M. Riener and D. A. Nicewicz, *Chem. Sci.*, 2013, **4**, 2625.
117 S. L. Mattes, H. R. Luss and S. Farid, *J. Phys. Chem.*, 1983, **87**, 4779–4781.
118 E. Hasegawa, T. Mukai and K. Yanagi, *J. Org. Chem.*, 1989, **54**, 2053–2058.
119 S. Hintz, J. Mattay, R. Van Eldik and W. F. Fu, *Eur. J. Org. Chem.*, 1998, 1583–1596.
120 B. D. Ravetz, N. E. S. Tay, C. L. Joe, M. Sezen-Edmonds, M. A. Schmidt, Y. Tan, J. M. Janey, M. D. Eastgate and T. Rovis, *ACS Cent. Sci.*, 2020, **6**, 2053–2059.
121 M. A. Ischay, Z. Lu and T. P. Yoon, *J. Am. Chem. Soc.*, 2010, **132**, 8572–8574.
122 C. L. Cruz and D. A. Nicewicz, *ACS Catal.*, 2019, **9**, 3926–3935.
123 A. F. Roesel, M. Ugandi, N. T. T. Huyen, M. Májek, T. Broese, M. Roemelt and R. Francke, *J. Org. Chem.*, 2020, **85**, 8029–8044.
124 A. J. Perkowski, C. L. Cruz and D. A. Nicewicz, *J. Am. Chem. Soc.*, 2015, **137**, 15684–15687.
125 S. K. Pedersen, A. Ulfkjær, M. N. Newman, S. Yogarasa, A. U. Petersen, T. I. Sølling and M. Pittelkow, *J. Org. Chem.*, 2018, **83**, 12000–12006.
126 H. Kwart and E. R. Evans, *J. Org. Chem.*, 1966, **31**, 410–413.
127 L. Buglioni, F. Raymenants, A. Slattery, S. D. A. Zondag and T. Noël, *Chem. Rev.*, 2022, **122**, 2752–2906.
128 S.-F. Wang, X.-P. Cao and Y. Li, *Angew. Chem., Int. Ed.*, 2017, **56**, 13809–13813.
129 F.-F. Tan, X.-Y. He, W.-F. Tian and Y. Li, *Nat. Commun.*, 2020, **11**, 6126.
130 J. C. Gonzalez-Gomez, N. P. Ramirez, T. Lana-Villarreal and P. Bonete, *Org. Biomol. Chem.*, 2017, **15**, 9680–9684.
131 E. Hasegawa, N. Izumiya, T. Fukuda, K. Nemoto, H. Iwamoto, S. Takizawa and S. Murata, *Tetrahedron*, 2016, **72**, 7805–7812.
132 Y. Pellegrin and F. Odobel, *C. R. Chim.*, 2017, **20**, 283–295.
133 M. A. Kellett, D. G. Whitten, I. R. Gould and W. R. Bergmark, *J. Am. Chem. Soc.*, 1991, **113**, 358–359.
134 M. Itoh, *J. Am. Chem. Soc.*, 1974, **96**, 7390–7394.
135 E. A. Chandross and J. Fercuson, *J. Chem. Phys.*, 1967, **47**, 2557–2560.
136 I. R. Gould, R. H. Young, L. J. Mueller and S. Farid, *J. Am. Chem. Soc.*, 1994, **116**, 8176–8187.
137 P. Herr, F. Glaser, L. A. Büldt, C. B. Larsen and O. S. Wenger, *J. Am. Chem. Soc.*, 2019, **141**, 14394–14402.
138 L. A. Büldt, X. Guo, R. Vogel, A. Prescimone and O. S. Wenger, *J. Am. Chem. Soc.*, 2017, **139**, 985–992.
139 C. E. McCusker and F. N. Castellano, *Chem. Commun.*, 2013, **49**, 3537–3539.

140 L. Pitzer, F. Sandfort, F. Strieth-Kalthoff and F. Glorius, *J. Am. Chem. Soc.*, 2017, **139**, 13652–13655.
141 T. Chinzei, K. Miyazawa, Y. Yasu, T. Koike and M. Akita, *RSC Adv.*, 2015, **5**, 21297–21300.
142 J. B. McManus, N. P. R. Onuska and D. A. Nicewicz, *J. Am. Chem. Soc.*, 2018, **140**, 9056–9060.
143 B. Zilate, C. Fischer and C. Sparr, *Chem. Commun.*, 2020, **56**, 1767–1775.
144 A. J. Rieth, M. I. Gonzalez, B. Kudisch, M. Nava and D. G. Nocera, *J. Am. Chem. Soc.*, 2021, **143**, 14352–14359.
145 Y. Qin, R. Sun, N. P. Gianoulis and D. G. Nocera, *J. Am. Chem. Soc.*, 2021, **143**, 2005–2015.
146 A. Aydogan, R. E. Bangle, A. Cadranel, M. D. Turlington, D. T. Conroy, E. Cauët, M. L. Singleton, G. J. Meyer, R. N. Sampaio, B. Elias and L. Troian-Gautier, *J. Am. Chem. Soc.*, 2021, **143**, 15661–15673.
147 S. Rafiq, B. Fu, B. Kudisch and G. D. Scholes, *Nat. Chem.*, 2021, **13**, 70–76.
148 N. Kandoth, J. Pérez Hernández, E. Palomares and J. Lloret-Fillol, *Sustainable Energy Fuels*, 2021, **5**, 638–665.
149 K. Goliszewska, K. Rybicka-Jasińska, J. A. Clark, V. I. Vullev and D. Gryko, *ACS Catal.*, 2020, **10**, 5920–5927.
150 A. Aydogan, R. E. Bangle, S. De Kreijger, J. C. Dickenson, M. L. Singleton, E. Cauët, A. Cadranel, G. J. Meyer, B. Elias, R. N. Sampaio and L. Troian-Gautier, *Catal. Sci. Technol.*, 2021, **11**, 8037–8051.
151 E. H. Spielvogel, B. G. Stevenson, M. J. Stringer, Y. Hu, L. A. Fredin and J. R. Swierk, *J. Org. Chem.*, 2022, **87**, 223–230.
152 L. Pause, M. Robert and J. M. Savéant, *J. Am. Chem. Soc.*, 1999, **121**, 7158–7159.
153 D. Y. Jeong, D. S. Lee, H. L. Lee, S. Nah, J. Y. Lee, E. J. Cho and Y. You, *ACS Catal.*, 2022, **12**, 6047–6059.
154 E. Vauthey, C. Högemann and X. Allonas, *J. Phys. Chem. A*, 1998, **102**, 7362–7369.
155 E. Vauthey, P. Suppan and E. Haselbach, *Helv. Chim. Acta*, 1988, **71**, 93–99.
156 T. Niwa, K. Kikuchi, N. Matsusita, M. Hayashi, T. Katagiri, Y. Takahashi and T. Miyashi, *J. Phys. Chem.*, 1993, **97**, 11960–11964.
157 S. L. Goldschmid, E. Bednářová, L. R. Beck, K. Xie, N. E. S. Tay, B. D. Ravetz, J. Li, C. L. Joe and T. Rovis, *Synlett*, 2022, **33**, 247–258.
158 S. De Kreijger, O. Schott, L. Troian-Gautier, E. Cauët, G. S. Hanan and B. Elias, *Inorg. Chem.*, 2022, **61**, 5245–5254.
159 P. A. Scattergood, A. Sinopoli and P. I. P. Elliott, *Coord. Chem. Rev.*, 2017, **350**, 136–154.
160 Y. Sasaki, N. Yanai and N. Kimizuka, *Inorg. Chem.*, 2022, **61**, 5982–5990.
161 D. A. W. Ross, P. A. Scattergood, A. Babaei, A. Pertegás, H. J. Bolink and P. I. P. Elliott, *Dalton Trans.*, 2016, **45**, 7748–7757.
162 S. A. E. Omar, P. A. Scattergood, L. K. McKenzie, C. Jones, N. J. Patmore, A. J. H. M. Meijer, J. A. Weinstein, C. R. Rice, H. E. Bryant and P. I. P. Elliott, *Inorg. Chem.*, 2018, **57**, 13201–13212.
163 A. R. Obah Kosso, N. Sellet, A. Baralle, M. Cormier and J.-P. Goddard, *Chem. Sci.*, 2021, **12**, 6964–6968.
164 K. Rybicka-Jasińska, T. Wdowik, K. Łuczak, A. J. Wierzba, O. Drapała and D. Gryko, *ACS Org. Inorg. Au*, 2022, **2**, 422–426.
165 M. Yang, S. Sheykhi, Y. Zhang, C. Milsmann and F. N. Castellano, *Chem. Sci.*, 2021, **12**, 9069–9077.
166 S. N. Sanders, M. K. Gangishetty, M. Y. Sfeir and D. N. Congreve, *J. Am. Chem. Soc.*, 2019, **141**, 9180–9184.
167 S. N. Sanders, T. H. Schloemer, M. K. Gangishetty, D. Anderson, M. Seitz, A. O. Gallegos, R. C. Stokes and D. N. Congreve, *Nature*, 2022, **604**, 474–478.
168 N. Sellet, M. Cormier and J.-P. Goddard, *Org. Chem. Front.*, 2021, **8**, 6783–6790.
169 C. J. Imperiale, P. B. Green, M. Hasham and M. W. B. Wilson, *Chem. Sci.*, 2021, **12**, 14111–14120.
170 J. Huang, J. Sun, Y. Wu and C. Turro, *J. Am. Chem. Soc.*, 2021, **143**, 1610–1617.